

Magnetic field induced charge instabilities in weakly coupled superlattices

R. Aguado^a and G. Platero

Departamento de Teoría de la Materia Condensada, Instituto de Ciencia de Materiales de Madrid, CSIC, Cantoblanco 28049, Madrid, Spain.

Using a time dependent selfconsistent model for vertical sequential tunneling, we study the appearance of charge instabilities that lead to the formation of electric field domains in a weakly coupled doped superlattice in the presence of high magnetic fields parallel to the transport direction. The interplay between the high non linearity of the system –coming from the Coulomb interaction– and the inter-Landau-level scattering at the domain walls (regions of charge accumulation inside the superlattice) gives rise to new unstable negative differential conductance regions and extra stable branches in the sawtooth-like I-V curves.

PACS numbers: 73.40.Gk, 72.15.Gd

Weakly coupled doped semiconductor superlattices are an example of non linear systems in which all intrinsic properties related to high non linearity such as multistability, spatio-temporal chaos, etc, can be externally modified : e.g. by the application of a bias voltage or by the variation of the doping densities in the wells or in the contacts. The strong non linear transport that results from the Coulomb interaction in these systems presents a rich variety of new physical phenomena: multistability and electric field domains formation [1–3], self sustained oscillations [4], bifurcation to chaos [5], etc. In particular, the current flowing through a weakly coupled doped semiconductor superlattice presents a complicated sawtooth structure with unstable regions of negative differential conductance and multistable regions. This structure of branches comes from the charge instabilities that appear due to the motion of the domain wall (accumulation layer) from one well to another. This motion, which is due to resonant tunneling between adjacent subbands, leads to the formation of electric field domains. In this Letter we study theoretically for the first time this phenomenon in the presence of high magnetic fields parallel to the transport direction. New physical questions that were not relevant in the absence of magnetic fields can be raised. In particular, what happens to the charge instabilities in the presence of the new energy scale in the problem, $\hbar\omega_c$?

Resonant tunneling through double barriers [6–10] and superlattices [11] in the presence of high magnetic fields has been widely studied. Also, dynamical instabilities and bifurcations to chaos induced by a magnetic field in a double barrier resonant tunneling diode have been recently predicted [12]. It is well known that the application of a magnetic field perpendicular to a two dimensional electron gas produces the formation of Landau levels. For ideal samples, the tunneling through the heterostructure conserves the Landau level index. However, due to interface roughness, impurity scatter-

ing, or phonon scattering, these conservation rules are relaxed and inter Landau level transitions take place [6–10]. Recent magnetotransport experiments on weakly coupled doped semiconductor superlattices performed by Schmidt *et al.* [13] show new unstable regions of negative differential conductance and extra stable branches in the I-V curves for a certain range of magnetic fields. In this work we will show how the interplay between the high non linearity of the system, and inter-Landau-level transitions through regions of charge accumulation in the structure –domain walls– can explain these new instabilities.

The main ingredients of our model are the following: we assume that the characteristic time for intersubband relaxation due to scattering which for optical phonon scattering is about 0.1 ps, is much smaller than the tunneling time. The latter is less than 0.5 ns, which is in turn much smaller than the dielectric relaxation time responsible for reaching a steady state, which is about 10 ns for the superlattices discussed in Ref. [4]. This separation of time scales, as well as the configuration of a typical sample, allows us to assume that only the ground state of each well is populated and that the tunneling processes are stationary. These assumptions then justify the use of rate equations for the electron densities at each well. In order to include relaxation in the transport direction due to the different scattering mechanisms, we suppose that the spectral densities in the quantum wells are Lorentzians whose half width γ is a parameter related to the scattering life time, which is of the order of picoseconds. Relaxation in the planes perpendicular to the transport is considered imposing current conservation in the stationary limit. This condition determines the sequential current as well as the Fermi energies within each well $\{\epsilon_{\omega_i}\}$ [14,15]. The electrons are described by a Fermi-Dirac distribution in each well, which implicitly assumes that some scattering mechanism thermalizes them towards a local equilibrium situation. In the absence of

such a mechanism for thermalizing the electrons the distribution functions are nonequilibrium objects and the rate equation is equivalent to a quantum kinetic method –i.e, Keldysh or Kadanoff-Baym, for example. The rate equations –for a given set $\{\epsilon_{\omega_i}\}$ – are:

$$\frac{dn_i}{dt} = J_{i-1,i} - J_{i,i+1} \quad i = 1, \dots, N. \quad (1)$$

In this equation, N is the number of wells, $J_{i,i+1}$ are the interwell currents and $J_{0,1}$ and $J_{N,N+1}$ are the currents through the contacts (emitter and collector regions). These currents are calculated by means of the Tunneling Hamiltonian method [14], and have dependencies $J_{i,i+1} \equiv J_{i,i+1}(\epsilon_{\omega_i}, \epsilon_{\omega_{i+1}}, \{\Phi\})$. $\{\Phi\}$ denotes the set of variables coming from the electrostatics: potential drops at the accumulation and depletion layers, barriers and wells, etc. These must be calculated selfconsistently for each applied bias. More details of the selfconsistent procedure and of the electrostatic model considered here are given in Ref. [15]. These rate equations, which include all of the relevant dynamics of the selfconsistent problem, can be rewritten in terms of an Ampère's law that explicitly shows the time-dependent current consisting of a displacement current plus a tunneling term [15] $\frac{\epsilon}{d} \frac{dV_i}{dt} + J_{i-1,i} = J(t)$. Here $\frac{V_i}{d}$ is the electric field at the i -th barrier and ϵ is the GaAs static permittivity. Nonetheless, in this work we restrict ourselves to the stationary regime $\frac{dn_i}{dt} \rightarrow 0$. In this limit, the interwell currents and the currents from the contacts are all equal to the total sequential current J . Following Ref. [15] and considering the formation of Landau levels in the planes perpendicular to the transport, we obtain the following expressions for the tunneling currents:

$$\begin{aligned} J_{0,1} &= \frac{e2g\hbar}{m^*2\pi} \sum_{j=1}^m \sum_{n=0}^{n_{max}^1} \int A_{Cj}^1(\epsilon_z) B_{1,2}(\epsilon_z) T_1(\epsilon_z) \\ &\quad \times [f_{\epsilon_F}(\epsilon_z) - f_{\epsilon_{\omega_1}}(\epsilon_z)] d\epsilon_z, \\ J_{i,i+1} &= \frac{e2g\hbar^3}{2\pi m^{*2}} \sum_{j=1}^m \sum_{n=0}^{n_{max}^i} \int A_{C1}^i(\epsilon_z) A_{Cj}^{i+1}(\epsilon_z) \\ &\quad \times B_{i,i+1}(\epsilon_z) B_{i+1,i+2}(\epsilon_z) T_{i+1}(\epsilon_z) \\ &\quad \times [f_{\epsilon_{\omega_i}}(\epsilon_z) - f_{\epsilon_{\omega_{i+1}}}(\epsilon_z)] d\epsilon_z, \\ J_{N,N+1} &= \frac{e2g\hbar}{m^*2\pi} \sum_{n=0}^{n_{max}^N} \int A_{C1}^N(\epsilon_z) B_{N,N+1}(\epsilon_z) T_{N+1}(\epsilon_z) \\ &\quad \times [f_{\epsilon_{\omega_N}}(\epsilon_z) - f_{\epsilon_F}(\epsilon_z + eV)] d\epsilon_z, \end{aligned} \quad (2)$$

In these expressions $f_{\epsilon_{\omega_i}}(\epsilon_z) = (1 + e^{\frac{(\epsilon_{\omega_i} - \epsilon_z - \epsilon(n))}{k_B T}})^{-1}$ are the Fermi functions, $\epsilon(n) = \hbar\omega_c(n + \frac{1}{2})$, $\omega_c = \frac{eB}{m^*}$ is the cyclotron frequency, n runs over all Landau levels below the Fermi energy of the region (emitter or i -th well) from which the electrons are tunneling. The Fermi

energies, ϵ_{ω_i} , must be calculated selfconsistently. Also, $g = \frac{eBS}{2\pi\hbar}$ is the factor of degeneracy for a given magnetic field B and area S , j labels the resonant state in each well i with energy ϵ_{Cj}^i , m is the total number of resonant states within the well contributing to the current and $B_{i,i+1} = k_i/(w + \alpha_i^{-1} + \alpha_{i+1}^{-1})$, where k_i and α_i are the wave vectors in the wells and the barriers, respectively. These depend on the local electric field. Finally, $T_i = 16k_{i-1}k_i\alpha_i^2 e^{-2\alpha_i d} (k_{i-1}^2 + \alpha_i^2)^{-1} (k_i^2 + \alpha_i^2)^{-1}$ is the dimensionless transmission probability through the i th barrier, and w and d are the well and barrier widths respectively.

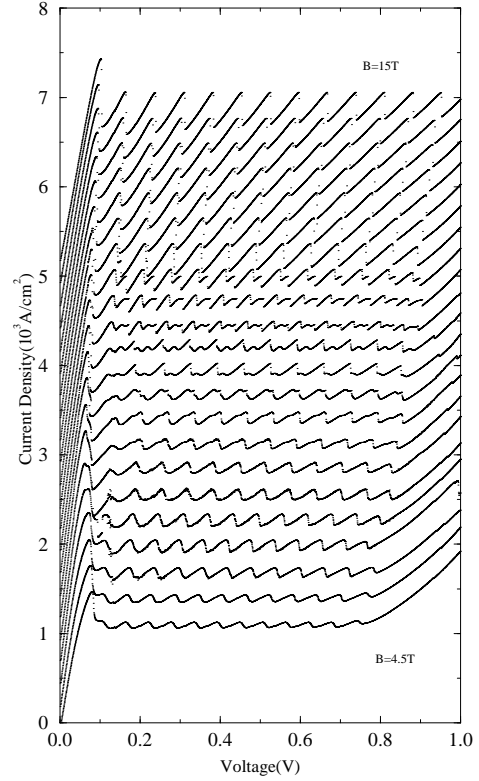


FIG. 1. I-V curves for different magnetic fields in increments of 0.5T. The curves are shifted in intervals of $0.2 \times 10^3 \frac{A}{cm^2}$ for clarity.

As we mentioned above, we use Lorentzians for the spectral densities in the wells $A_{Cj}^i(\epsilon) = \gamma/[(\epsilon - \epsilon_{Cj}^i)^2 + \gamma^2]$. Although this assumption can be improved by performing a calculation of the self-energies including microscopically the scattering (i.e., including the energy and magnetic field dependence of the selfenergy), previous microscopic calculations of impurity scattering in the presence of magnetic fields have shown this Lorentzian form to be a good approximation [8]. On the other hand, our hamiltonian restricts inter Landau level scattering just within

the wells. The effect of this contribution on the current has been shown to be the most important one of the possible impurity scattering [8] and interface roughness [9] contributions in a double barrier.

Thus, our phenomenological model for the scattering accounts for the main physics: inter-Landau-level scattering at the domain wall (see below), and makes the non linear problem tractable numerically. Also it is important to emphasize that the Fermi energies in each well are variables; i.e., after each tunneling event the lateral energy $\epsilon(n)$ is not necessarily conserved. After reaching a stationary state, at a certain bias, some amount of charge is accumulated in the well where the domain wall is formed. Depending on the degeneracy, it could imply an increase in the maximum Landau level occupied in one well with respect to its neighboring. The interwell tunneling then could involve processes where $\Delta n = n_{max}^{i+1} - n_{max}^i \neq 0$.

We have analyzed a superlattice consisting of 15 wells of GaAs of 90 Å thickness and GaAlAs barriers 50 Å wide. The emitter doping is $N_D = 2 \times 10^{18} \text{cm}^{-3}$ and the doping in the wells is $N_D^w = 1.5 \times 10^{11} \text{cm}^{-2}$, with $\gamma = 4 \text{meV}$, and $T = 0 \text{K}$. For zero temperature the expression for the charge density in the i -th well is analytic: $n_i = \frac{em^* \omega_c}{\pi^2 \hbar} \sum_{n=0}^{n_{max}^i} \left[\arctg\left(\frac{\epsilon_{\omega_i} - \epsilon(n) - \epsilon_{C1}^i}{\gamma}\right) - \arctg\left(\frac{-\epsilon_{C1}^i}{\gamma}\right) \right]$. In Fig. 1 the I-V curve is plotted for different magnetic fields (the curves are shifted in the abscissa axis for clarity). For low magnetic fields, we observe a main peak at low bias coming from ground to ground state interwell tunneling, and a sawtooth structure at high bias due to electric field domains formation. As the magnetic field increases, additional unstable negative differential conductance and stable branches show up in the current density.

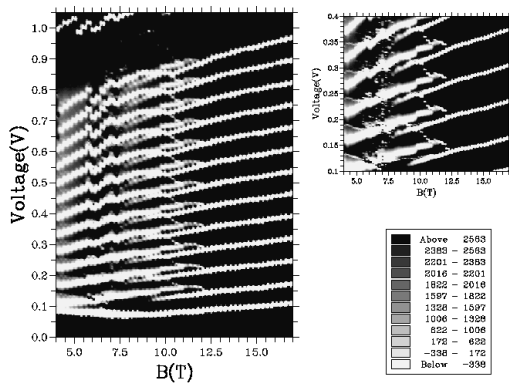


FIG. 2. Differential conductivity versus bias voltage and magnetic field.

This extra structure disappears as the magnetic field is increased above $\sim 13 \text{T}$. In order to study the range where this effect manifests itself in more detail, we plot

in Fig. 2 a contour plot of the differential conductivity as a function of B and the external bias V (negative differential conductance regions are the white lines).

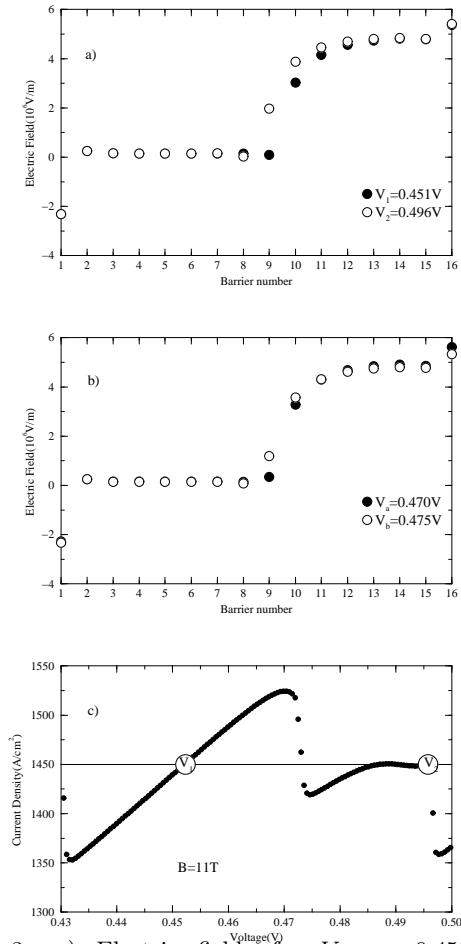


FIG. 3. a) Electric fields for $V_1 = 0.451 \text{V}$ and $V_2 = 0.496 \text{V}$, b) Electric fields for $V_a = 0.470 \text{V}$ and $V_b = 0.475 \text{V}$, c) Detail of the I-V curve for $B = 11 \text{T}$ showing the extra branch.

One can see that the additional structure in the current takes place between 8 and 12.5 T where the differential conductivity shows two branches at fixed magnetic field that repeat periodically. This result is in good qualitative agreement with experiment, that shows this effect up to 19 T [13]. At lower magnetic fields around 6.5 Tesla, and voltages close to 0.4 Volt, there is a small structure reflecting the formation of a multistable solution (see Fig. 2). Our calculations have been performed by direct numerical integration of the dynamical system [15] in order to permit a direct comparison with the experiment [13]. The experimental I-V curves have been obtained by sweeping the DC bias only in one direction –i.e., by increasing the DC bias in between the emitter and the collector. Nonetheless, it is possible to use more complicated numerical techniques such as the numerical continuation method [15] in order to obtain all of the unstable and multistable regions. The multistable regions

for the current could be observed in the experimental curves along up and down voltage sweeps.

We shall concentrate in one region of bias for the current density and fix $B=11\text{T}$ in order to obtain an explanation for these new structures appearing at intermediate magnetic fields. We plot in Fig. 3c, a blow up of the current for $B=11\text{T}$ in the region of voltages where one third of the wells already belongs to the high field domain. We have analyzed the electric field distribution for two different biases that give the same current density: $V_1 = 0.451\text{V}$ and $V_2 = 0.496\text{V}$ (see Fig. 3a). The first voltage V_1 , corresponds to a current solution that belongs to the first branch and the second one V_2 , corresponds to a solution in the second branch (Fig. 3c).

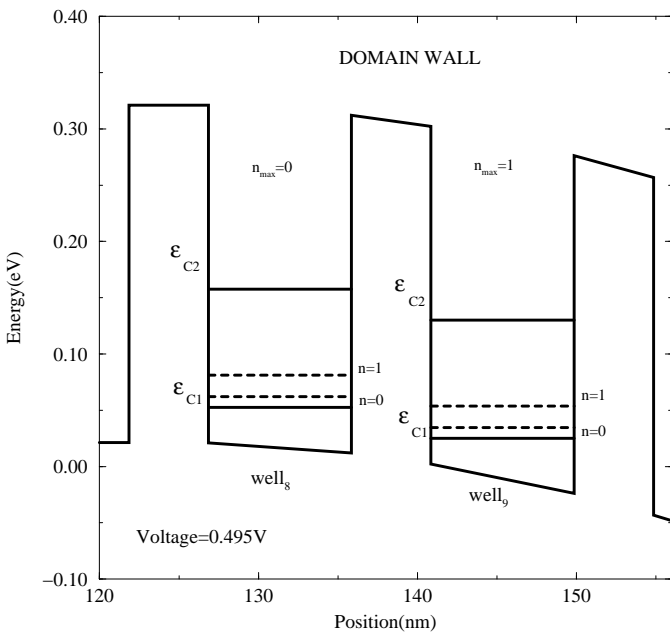


FIG. 4. Detail of the calculated electrostatic profile for 0.495 Volt and $B=11\text{T}$. Dotted lines are the Landau levels. Also the calculated maximum occupied Landau levels for each well are shown.

As we can see, the current density presents a discontinuity at $V_a = 0.47\text{V}$, and it drops abruptly. Increasing the voltage, an additional branch shows up. The current decreases from one branch to the next due to the electric field distribution (see in Fig. 3b the electric field distribution in the neighborhood of the current discontinuity). For voltages higher than $V_a = 0.47\text{V}$ the resonant states in neighbor wells at the domain wall become disaligned in energy, their wavefunctions overlap decreases,

and the current decreases as well. The current discontinuity between both branches is due to the strongly non linear charge and field distributions. The electric field is discontinuous between $V_a = 0.47\text{V}$ and $V_b = 0.475\text{V}$ at the 9th barrier (Fig. 3b). A detail of the calculated potential profile for a voltage slightly less than V_2 (Fig. 4) shows the electrostatic profile at the domain wall region. This voltage corresponds to the formation of the extra branch. The position of the resonant states—which have been drawn as discrete ones for simplicity—and Landau levels energies at the domain wall are depicted as continuous and dotted lines respectively. Also, the calculated maximum Landau level partially occupied in each well, $n_{max}^8=0$ and $n_{max}^9=1$ respectively are indicated. These are obtained from the calculated Fermi levels for this voltage. We conclude that the extra branch of the current is a result of inter Landau level transition at the domain wall, $\Delta n = n_{max}^9 - n_{max}^8 = 1$, between the 8th and 9th wells. In this situation, the electrons tunnel from a region with low charge density accumulation towards the domain wall while changing their maximum parallel energy to $\hbar\omega_c(n_{max}^9 + \frac{1}{2})$. As the DC voltage increases, the domain wall moves from one well to the previous one—in this particular case from the 9th well to the 8th well—and the structure discussed above repeats periodically (see Fig.1). For magnetic fields below 8 Tesla, the motion of the domain wall does not involve a change in the maximum occupied Landau level and there is no inter Landau level scattering involved. In the regime of high magnetic fields, where the domain boundary enters the magnetic quantum limit, the lowest Landau level is the only one occupied in the wells because high degeneracy, and we obtain only one branch which repeats periodically as the domain wall moves.

The reason why we do not obtain exactly the same range of magnetic fields as in experiment [13], is mainly due to the simplicity of our model for scattering as we have discussed above. We have observed that by increasing the doping in the wells, the range of magnetic fields becomes closer to the experimental one. Furthermore, we have not included spin-splitting and exchange effects in the calculation. At high fields, the exchange could be important and the spin splitting must be considered. This effect would also give new features in the non linear current at high fields. This will be addressed in future work.

In summary, we have proposed and solved a dynamical selfconsistent model for studying the sequential transport through a doped superlattice in the presence of magnetic fields. We study the appearance of charge instabilities leading to the formation of electric field domains. For intermediate magnetic fields, the appearance of new unstable negative differential conductance regions and new stable branches in the sawtooth-like I-V curves is discussed. These new features in the current can be explained in terms of inter Landau level scattering occurring at the domain walls.

One of us (G.P.) acknowledges Prof. K. Von Klitzing for addressing us to this problem and for very interesting comments and a critical reading of the manuscript. Also G.P. acknowledges him and his departament for their hospitality at MPI in Stuttgart where this work was initiated. We acknowledge as well Dr T. Schmidt for several discussions on his experimental results prior to publication, Dr. L. Brey for interesting discussions, Dr. J.P. Rodriguez for a critical reading of the manuscript and Prof. L.L. Bonilla and Dr. M. Moscoso for collaboration in related topics.

(a) Present Address: Department of Applied Physics, Delft University of Technology, Delft, The Netherlands.

-
- [1] H. T. Grahn, R. J. Haug, W. Müller, and K. Ploog, Phys. Rev. Lett., **67**, 1618 (1991).
 - [2] S. H. Kwok, R. Merlin, H. T. Grahn, and K. Ploog, Phys. Rev. B, **50**, 2007 (1994).
 - [3] A. Wacker, M. Moscoso, M. Kindelán, and L. L. Bonilla, Phys. Rev. B, **55**, 2466 (1997).
 - [4] J. Kastrup, R. Klann, H. T. Grahn, K. Ploog, L. L. Bonilla, J. Galán, M. Kindelán, M. Moscoso, and R. Merlin, Phys. Rev. B, **52**, 13761 (1995).
 - [5] O. M. Bulashenko and L. L. Bonilla, Phys. Rev. B, **52**, 7849 (1995).
 - [6] M. L. Leadbeater et al, Phys. Rev. B, **39**, 3438 (1989); L. Eaves et al., Appl. Phys. Lett., **52**, 212 (1988); C. H. Yang, M. J. Yang and Y. C. Kao, Phys. Rev. B, **40**, 6272 (1989).
 - [7] G. S. Boebinger, A. F. J. Levi, S. Schmitt-Rink, A. Passner, L. N. Pfeiffer and K. W. West, Phys. Rev. Lett., **65**, 235 (1990).
 - [8] H. A. Fertig, Song He and S. Das Sarma, Phys. Rev. B, **41**, 3596 (1990).
 - [9] J. Leo and A.H. MacDonald, Phys. Rev. B, **43**, 9763 (1991).
 - [10] N. Zou et al., Phys. Rev. Lett., **71**, 1756 (1993).
 - [11] W. Müller, H. T. Grahn, R. J. Haug and K. Ploog, Phys. Rev. B, **46**, 9800 (1992) and references therein.
 - [12] P. Orellana, E. Anda, and F. Claro, Phys. Rev. Lett., **79**, 1118 (1997).
 - [13] T. Schmidt, Phd Thesis, Max Planck Institut FKF, Stuttgart (1997); T. Schmidt et al., to be published.
 - [14] M. Jonson, Phys. Rev. B, **39**, 5924 (1989).
 - [15] R. Aguado, G. Platero, M. Moscoso and L. L. Bonilla, Phys. Rev. B (RC), 16053 (1997).